MINERAL SOLUBILITY AND WEATHERING RATE CONSTRAINTS ON METAL CONCENTRATIONS IN GROUND WATERS OF MINERALIZED AREAS NEAR QUESTA, NEW MEXICO[1]

D. Kirk Nordstrom,[2] and R. Blaine McCleskey[3]

Abstract. The U.S. Geological Survey, in cooperation with the New Mexico Environment Department, has completed a 4-year investigation (2001-2005) to determine the pre-mining ground-water quality at Molycorp's Questa molybdenum mine in northern New Mexico. Current mine-site ground waters are often contaminated with mine-waste leachates and no data exists on pre-minng ground-water quality so that pre-mining conditions must be inferred. Ground-water quality undisturbed by mining is often worse than New Mexico standards and data are needed to help establish closure requirements. The key to determining pre-mining conditions was to study the hydrogeochemistry of a proximal natural analog. Main rock types exposed to weathering include a Tertiary andesite and the Tertiary Amalia tuff (rhyolitic composition), both hydrothermally altered to various degrees. Two types of ground water are common in mineralized areas, acidic ground waters in alluvial debris fans with pH 3-4 and bedrock ground waters with pH 6-8. Siderite, ferrihydrite, rhodochrosite, amorphous to microcrystalline $Al(OH)_3$, calcite, gypsum, barite, and amorphous silica mineral solubilities control concentrations of Fe(II), Fe(III), Mn(II), Al, Ca, Ba, and SiO_2, depending on pH and solution composition. Concentrations at low pH are governed by element abundance and mineral weathering rates. Concentrations of Zn and Cd range from detection up to about 10 and 0.05 mg/L, respectively, and are derived primarily from sphalerite dissolution. Concentrations of Ni and Co range from detection up to 1 and 0.4 mg/L, respectively, and are derived primarily from pyrite dissolution. Concentrations of Ca and SO_4^{-2} are derived from secondary gypsum dissolution and weathering of calcite and pyrite. Metal:sulfate concentration ratios are relatively constant for acidic waters, suggesting consistent weathering rates. These trends, combined with lithology, mineralogy, and mineral solubility controls, provide useful constraints on pre-mining ground-water quality for the mine site where the lithology is known.

[1] Paper presented at the 7th International Conference on Acid Rock Drainage (ICARD), March 26-30, 2006, St. Louis MO. R.I. Barnhisel (ed.) Published by the American Society of Mining and Reclamation (ASMR), 3134 Montavesta Road, Lexington, KY 40502

[2] D. Kirk Nordstrom, Research Hydrogeochemist, US Geological Survey, Boulder, CO, 80303, R. Blaine McCleskey, Research Chemist, US Geological Survey, Boulder, CO, 80303

7th International Conference on Acid Rock Drainage, 2006 pp 1383-1399
DOI: 10.21000/JASMR06021383
http://dx.doi.org/10.21000/JASMR06021383

Introduction

Active and inactive mine sites are challenging to remediate because of their complexity and scale. Regulations meant to achieve environmental restoration at mine sites are equally challenging to apply for the same reasons. The goal of environmental restoration is to restore contaminated mine sites, as closely as possible, to pre-mining conditions. Metalliferous mine sites in the western U.S. are commonly located in hydrothermally altered and mineralized terrain in which pre-mining metal concentrations of soil, sediment, and water were already high. Unfortunately, those pre-mining concentrations were not normally measured or documented but they can sometimes be reconstructed using scientific inference.

Molycorp's Questa molybdenum mine in the Red River Valley, northern New Mexico, must meet several requirements on closure including a return of ground-water quality to New Mexico's ground-water quality standards unless it can be shown that concentrations before mining were higher than the standards. Ground waters at the mine site were not chemically analyzed before mining began. The U.S. Geological Survey (USGS), in cooperation with the New Mexico Environment Department, has completed a 4-year investigation (2001-2005) on the baseline and pre-mining ground-water quality at Molycorp's Questa molybdenum mine site. The area of investigation, shown in Fig. 1, included the Red River Valley from the town of Red River to the USGS stream-flow gauging station at the US Forest Service District Ranger Station near the town of Questa. The aim of this investigation was to infer the pre-mining ground-water quality by examining the geologic, hydrologic, and geochemical controls on ground-water quality at a proximal analog site near the Questa Molybdenum mine. Among several useful approaches that could be used to estimate pre-mining water quality (Runnells et al., 1992; Alpers and Nordstrom, 2000), the most direct one is the proximal analog. The most useful proximal analog should be similar to the mine site in lithology, geologic structure, topography, hydrology, climate, and ground-water characteristics. The site chosen for the proximal analog is the Straight Creek catchment, located within the study area approximately 3 miles to the east of the eastern boundary of the mine site (Fig. 2).

Geologic studies for this project include mapping of surface mineralogy by Airborne Visible-Infrared Imaging Spectrometry (AVIRIS; Livo and Clark, 2002); bedrock fractures and their potential effect on ground-water flow (Caine, 2003; J.S. Caine, USGS, written communication, 2005); depth to bedrock measurements (Powers and Burton, 2004), leaching studies of scars and waste-rock piles (K. Smith, USGS, written communication, 2005); mineralogy and mineral chemistry and its potential effect on ground-water quality (Plumlee et al., 2005); environmental geology and debris-flow hazards of the Red River Valley (Ludington et al., 2004); lake sediment chemistry (Church et al., 2005); and geomorphology and its effect on ground-water flow (K. Vincent, USGS, written communication, 2005). Hydrologic studies for this project include compilations of historical surface- and ground-water quality data (LoVetere et al., 2004; Maest et al., 2004); synoptic/tracer studies with mass loading and other water-quality trends of the Red River (McCleskey et al., 2003; B. Kimball, K. Nordstrom, R. Runkel, K. Vincent, and P. Verplanck, USGS, written communication, 2005); reaction-transport modeling of the Red River (Ball et al., 2005); hydrology and water balance for the Red River Valley (C. Naus and D. McAda, USGS, written communication, 2005); ground-water geochemistry of selected wells undisturbed by mining in the Red River Valley (Naus et al., 2005; Nordstrom et al., 2005); and quality assurance and quality control of water analyses (McCleskey et al., 2004). A listing of Questa baseline and pre-mining ground-water quality reports is online (Questa, 2005). This

paper focuses on the interpretation of natural ground-water quality in mineralized areas of the Red River Valley. Specifically, the water-rock interactions that govern the composition of ground waters for mineralized areas outlined in this paper also should apply to pre-mining ground-water quality at Molycorp's Questa mine site.

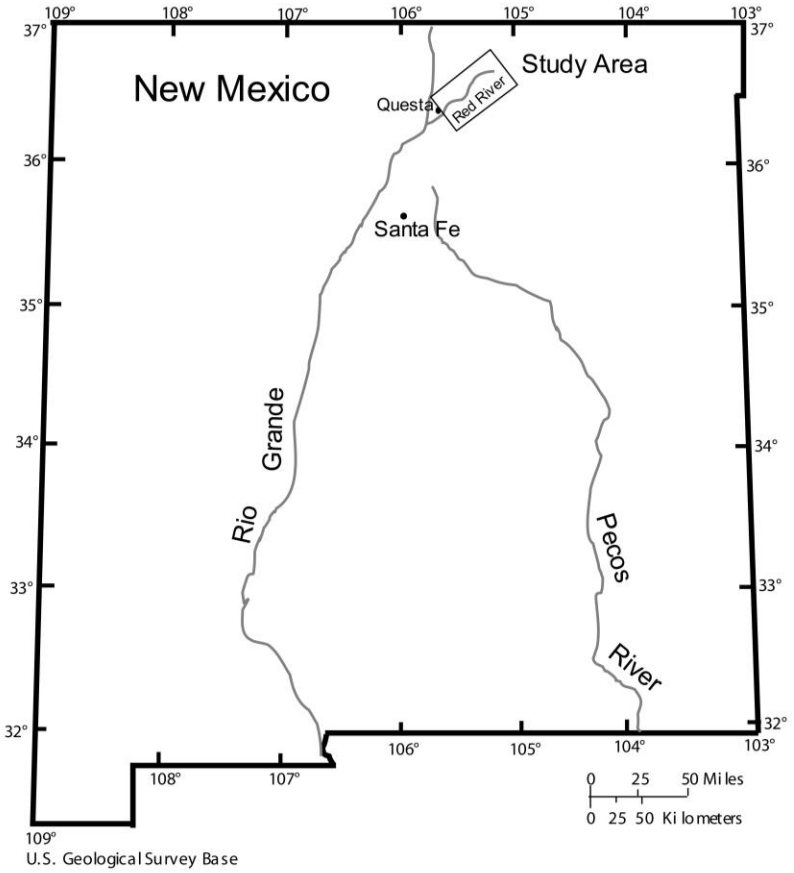

Figure 1. Location of the Red River, New Mexico.

The Red River Valley is located in the Taos Range of the Sangre de Cristo Mountains in northern New Mexico and southern Colorado. The main rock types are a basement of Precambrian granitic and metamorphic rocks, overlain by Tertiary andesite and the Tertiary Amaila Tuff, and intruded by granitic stocks that caused hydrothermal alteration of the volcanics (Meyer and Leonardson, 1990; Ludington et al., 2004). Hydrothermal alteration has resulted in potassic alteration, magnetite-hematite-quartz stockwork veining, fluorite-carbonate veining, quartz-sericite-pyrite alteration (QSP), quartz-sericite alteration (QS, sulfide-poor), argillic alteration, and propylitic alteration. Carbonate veining and alteration includes calcite, dolomite, rhodochrosite, and magnesite (Plumlee et al., 2005; Molycorp, oral communication, 2005). The valley follows a portion of the Questa caldera margin and has extensive mineralized areas, steep topography, and rapidly forming debris fans. Many of these debris fans are forming from "scar" areas of intense QSP alteration with such rapid erosion rates that vegetation cannot grow. A three-dimensional view of the valley is shown in Fig. 2 with the mine site and several scar areas shown as barren outcrops.

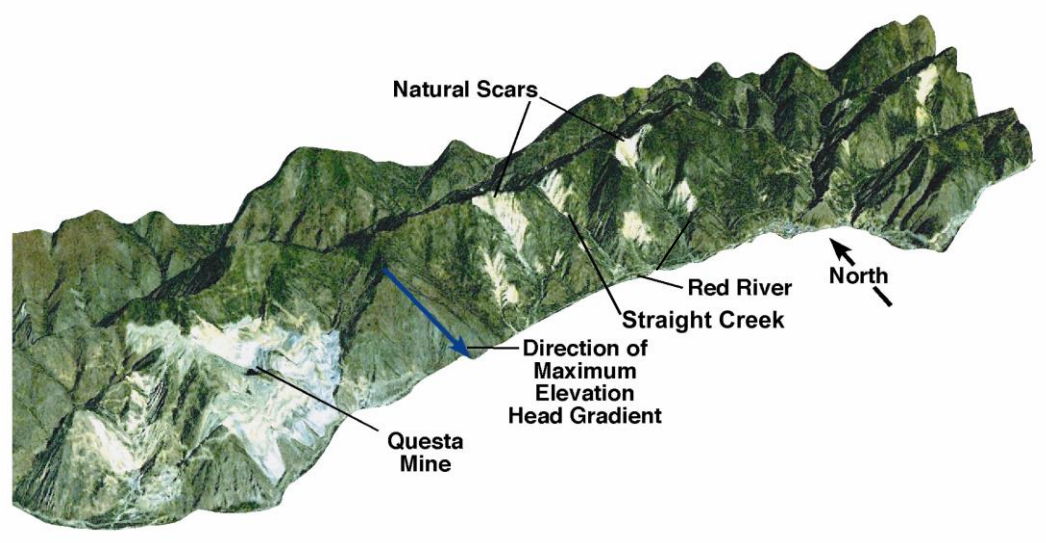

Figure 2. Three-dimensional natural color satellite image on a USGS digital elevation model for the northern section of the Red River Valley between Molycorp's Questa mine site and the town of Red River showing natural scars (from J.S. Caine, USGS, written communication, 2005).

A detailed hydrogeochemical investigation was completed on Straight Creek, a proximal analog site (Naus et al., 2005). Ground-water wells were completed in the Straight Creek debris fan, tapping both the alluvial and bedrock aquifers (Fig. 3). The results from chemical analyses of these ground waters and the Straight Creek surface waters that feed the alluvial aquifer provided the framework for the following interpretations, but additional water samples were collected from other mineralized catchments undisturbed by mining activities to broaden the applicability of the results.

Methods

Ground-water samples were collected (2001-2003) using bladder pumps specifically designed for purging and sampling at low flow rates. For most wells, a unique stabilization/purging time was established by monitoring iron redox concentrations, pH, specific conductance, Eh, and dissolved oxygen (Naus et al., 2005; Nordstrom et al., 2005).

Field measurements were obtained by pumping water through a flow-through cell containing pH, Eh, temperature, and dissolved O_2 electrodes and probes. Ground-water samples were routinely collected by filtering the water through a disposable capsule filter having a nominal pore size of 0.45 µm (Naus et al., 2005; Nordstrom et al., 2005). Several sample splits were collected for analyses of inorganic constituents and redox species. Samples for the determination of major cations and trace metals (As, Al, B, Ba, Be, Bi, Ca, Cd, Ce, Co, Cr, Cs, Cu, Dy, Er, Eu, Fe, Gd, Hf, Ho, K, La, Li, Lu, Mg, Mn, Mo, Na, Nd, Ni, Pb, Pr, Rb, Re, Sb, Se, SiO_2, Sm, Sr, Ta, Tb, Te, Th, Tl, Tm, U, V, W, Y, Yb, Zr, and Zn), major anions (Br, Cl, F, NO_3, and SO_4), alkalinity, and dissolved organic carbon (DOC) were filtered and then stabilizing reagents, if needed, were added. Sample bottles were pre-rinsed with filtered water prior to sample collection. Analytical methods are described in Naus et al. (2005). Quality assurance and quality control of water analyses included duplicate sampling, sequential filtration studies, filter

pore size comparisons, analyses of blanks, spike recoveries, analyses by different methods, and analyses by different laboratories (McCleskey et al., 2004).

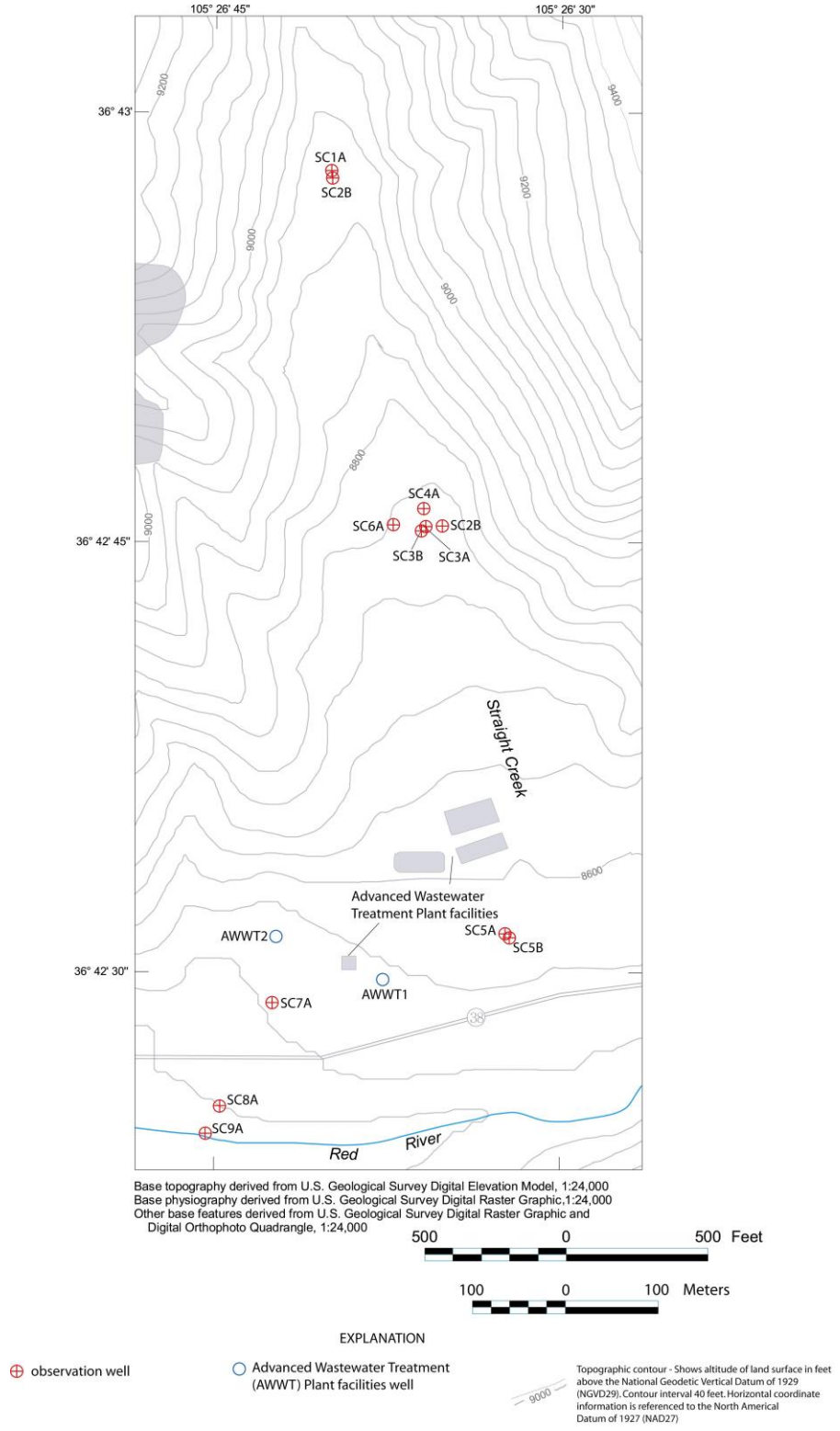

Figure 3. Map showing locations of wells in the Straight Creek catchment.

Results and Discussion

The Straight Creek alluvial aquifer is fed by acid rock drainage (pH 2.5 to 3) from the Straight Creek scar and is progressively diluted as it moves downgradient. Sulfate concentrations decreased from about 2,100 mg/L in the most up-gradient well to less than 1,000 mg/L in the most downgradient well as shown in Fig. 4. This trend suggested that constituents with conservative (i.e. non-reactive) behavior could be distinguished from those that were reactive by plotting the concentration of each in relation to sulfate concentration and testing the correlations for linear or non-linear trends. A strong linear correlation with SO_4^{-2} should indicate the constituent was predominantly conservative and a poor correlation or non-linearity should indicate the constituent was predominantly non-conservative. A bedrock aquifer is also fed by infiltrating acid waters, but these are of circumneutral pH because they are anoxic and cannot oxidize pyrite and they are buffered by carbonate minerals, primarily calcite.

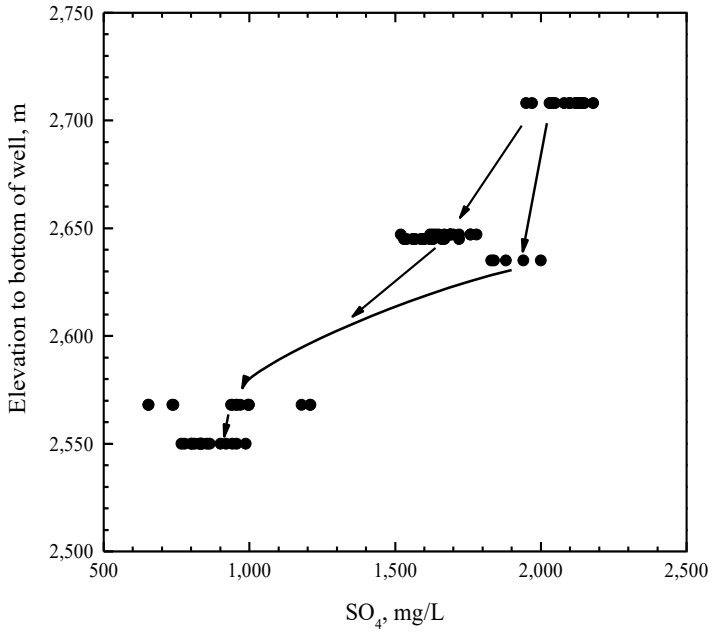

Figure 4. Ground-water elevation plotted relative to sulfate concentrations for the Straight Creek alluvial aquifer. Arrows indicate direction of water flow.

The primary determinant of whether a dissolved constituent behaves conservatively or non-conservatively is the pH because most metal solubilities are strongly affected by hydrolysis, which is a function of pH. Mineral precipitation and sorption reactions are often inhibited at low pH. The correlations of constituent concentrations relative to SO_4^{-2} concentrations demonstrated that most constituents behaved conservatively in the alluvial aquifer, not surprising for the pH range of 3 to 4. The trace elements Zn, Cd, Ni, and Co behave conservatively. In Fig. 5A, Zn concentrations are plotted relative to SO_4^{-2}concentrations and in Fig. 5B the Cd concentrations are plotted relative to Zn concentrations. Both correlation coefficients are greater than 0.9 and

the strong correlation between cadmium and zinc ($r^2 = 0.96$) suggests they might be derived from the same mineral. Indeed, the dominant source for both cadmium and zinc is sphalerite, ZnS, and Zn:Cd weight ratios in sphalerite range typically from 50-200 (Fleischer, 1955). The same range of Zn:Cd weight ratios was found for sphalerites from mineralized areas in the Red River Valley (Plumlee et al., 2005) and the average weight ratio for the correlation trend in Fig. 5B is 180. Hence, the available evidence points to weathering of sphalerite as the primary source of Zn and Cd in the Red River Valley and in pre-mining acidic ground waters of Molycorp's Questa mine site.

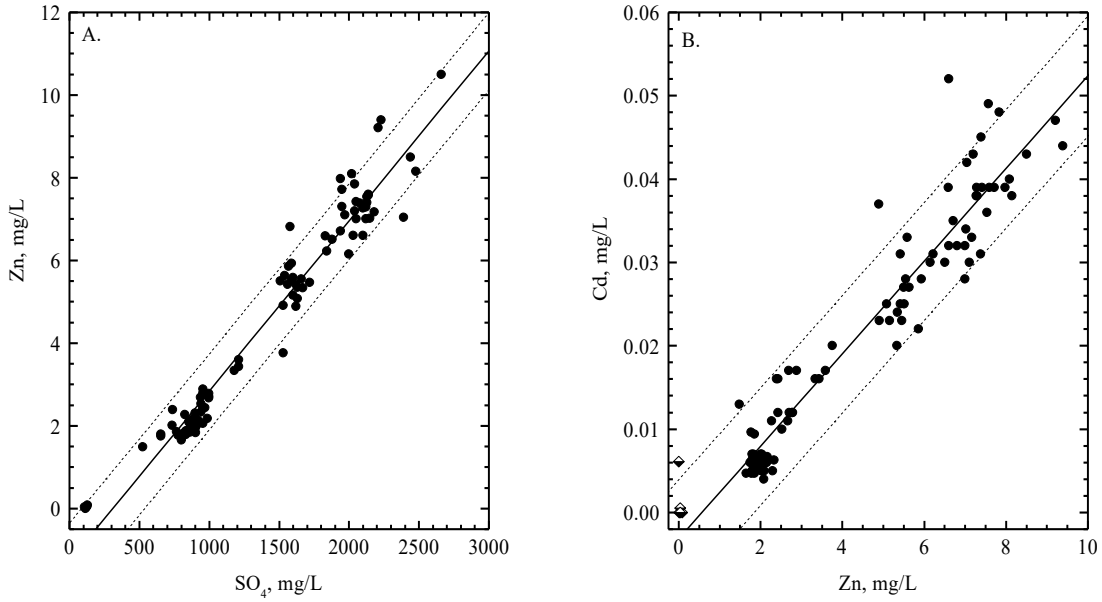

Figure 5. A. Concentrations of Zn relative to sulfate for Straight Creek surface and alluvial ground waters (pH = 2.5 to 4). B. Concentrations of Cd relative toZn for Straight Creek surface and alluvial ground waters.

Another example of conservative behavior in acidic waters is shown for Ni and Co concentrations in Fig. 6. Nickel concentrations correlate strongly with SO_4^{-2} concentrations as shown in Fig. 6A. The correlation of Co with Ni ($r^2 = 0.98$) is the second strongest of all correlations that have been obtained is shown in Fig. 6B. The strongest correlation ($r^2 = 0.99$, data not shown) is between Zn and Mn. Studies on mineral chemistry indicate that the primary source of Ni and Co is from pyrite, especially pyrite found in altered andesite (Plumlee et al., 2005).

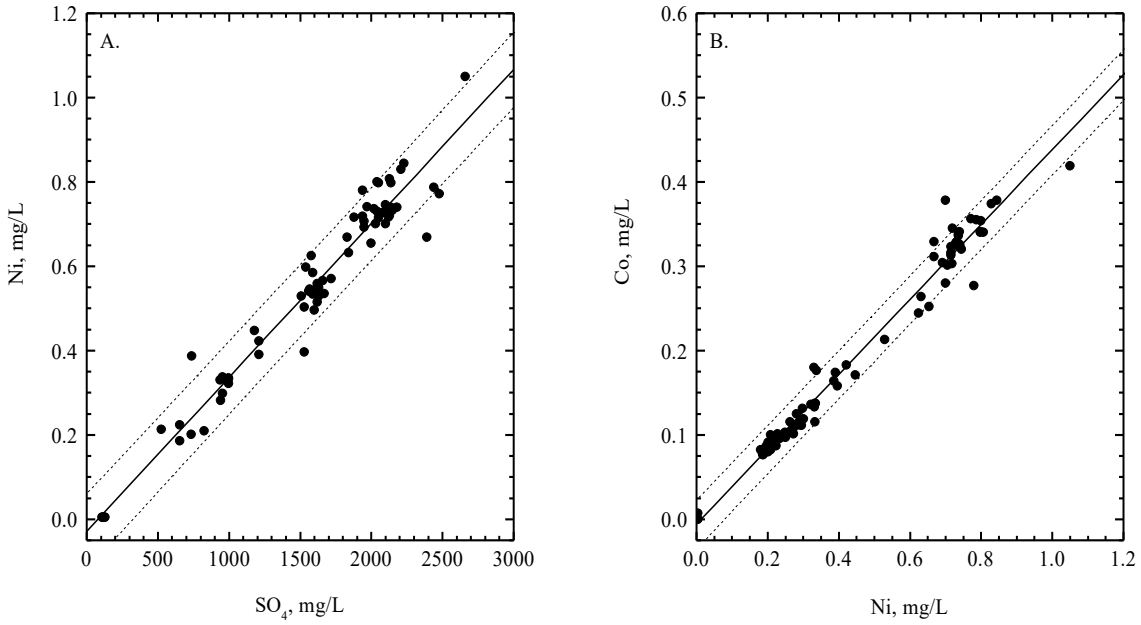

Figure 6. A. Concentrations of Ni relative to sulfate for Straight Creek surface and alluvial ground waters (pH = 2.5 to 4). B. Concentrations of Co relative to Ni for Straight Creek surface and alluvial ground waters.

Several constituents show distinctly non-conservative behavior at pH values greater than 4 but iron shows non-conservative behavior at even lower pH values. The correlation between iron and sulfate concentrations is poor, but if Fe^{+3} and Fe^{+2} iron concentrations are examined separately geochemical trends become apparent. Ferric iron concentrations range widely from greater than 100 mg/L to less than 10 µg/L depending on pH. In the following plots, data from all wells are used so that the full range of pH can be seen. These samples include acidic alluvial well waters and neutral-pH bedrock well waters. Most of the trace elements have very low concentrations in the neutral-pH ground waters.

A log plot of Fe^{+3} iron concentrations relative to pH (also a log scale) reflects an inverse linear trend (Fig. 7A). Dissolved Fe^{+3} iron concentrations for pH values greater than 5, although covering a range in concentration from 1 to 1,000 µg/L, have been shown to be below the detection limits of the colorimetric (FerroZine) method (To et al., 1999; Nordstrom et al., 2005). In this circumneutral pH range, iron colloids (hydrous ferric oxides or HFOs) are small enough to pass through filtration media and contribute to the apparent measurement of dissolved Fe^{+3} iron. If these measurements are eliminated from the database and the saturation indices (SI) for ferrihydrite (a proxy for a mixture of HFOs) are plotted relative to total dissolved iron concentrations, a solubility control is maintained at ferrihydrite saturation (pK = 3 to 4.9, Fig. 7B). Hence, Fe^{+3} iron concentrations appear to be controlled by ferrihydrite-like solubility.

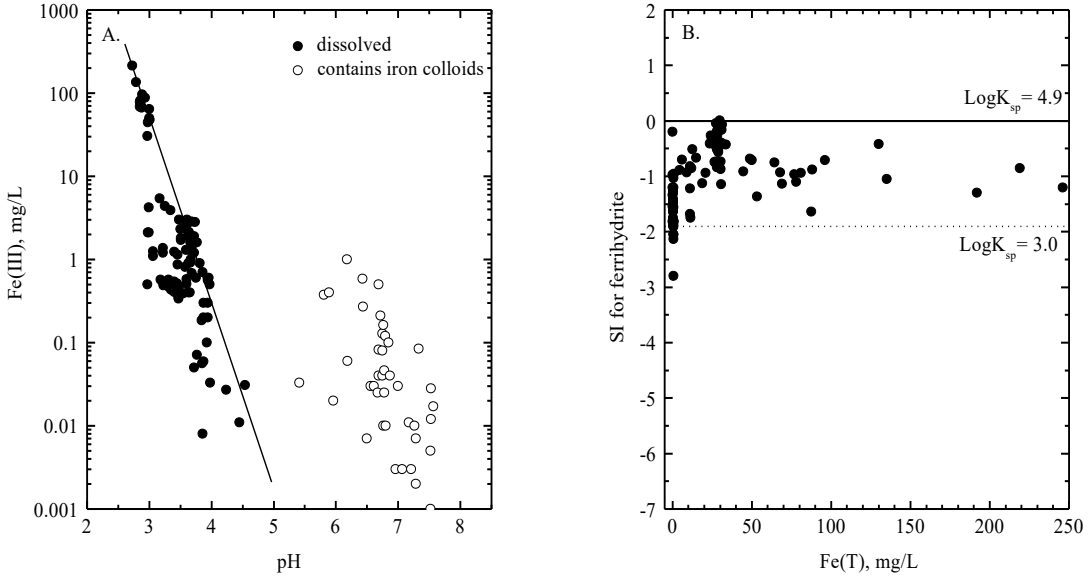

Figure 7.A. Logarithm of ferric iron concentration (Fe(III)) plotted relative to pH for both acidic and neutral-pH ground waters from the Red River Valley. The straight line is drawn through data points representing samples that have reached saturation with respect to ferrihydrite. B. SI for ferrihydrite plotted relative to total dissolved Fe concentration (Fe(T)).

Ferrous iron concentrations have been shown to reach siderite, $FeCO_3$, saturation in the study area (Nordstrom et al., 2005). If siderite saturation limits ferrous iron concentrations because of the common-ion effect, a plot of Fe^{+2} iron concentrations relative to alkalinity should follow an inverse correlation and this trend is apparent in Fig. 8A. The slight increase in Fe^{+2} iron concentration shown at the highest concentrations of alkalinity may reflect formation of a $Fe(CO_3)_2^{-2}$ complex. Saturation indices for siderite plotted in Fig. 8B show that saturation is reached only when pH values are at least 6. The highest SI values for siderite are those at the highest pH values, also consistent with the possible formation of a $Fe(CO_3)_2^{-2}$ complex.

Similarly to siderite, Mn concentrations should vary inversely with increasing alkalinity concentrations and they do as shown in Fig. 9A. Note that the trend is similar to that for Fe^{+2} iron concentrations in that the Mn concentrations are slightly higher at the highest alkalinities than at the medium range of alkalinities, suggesting the formation of a $Mn(CO_3)_2^{-2}$ complex. Saturation indices for rhodochrosite (Fig. 9B) show that saturation is reached only when pH values are at least 6.

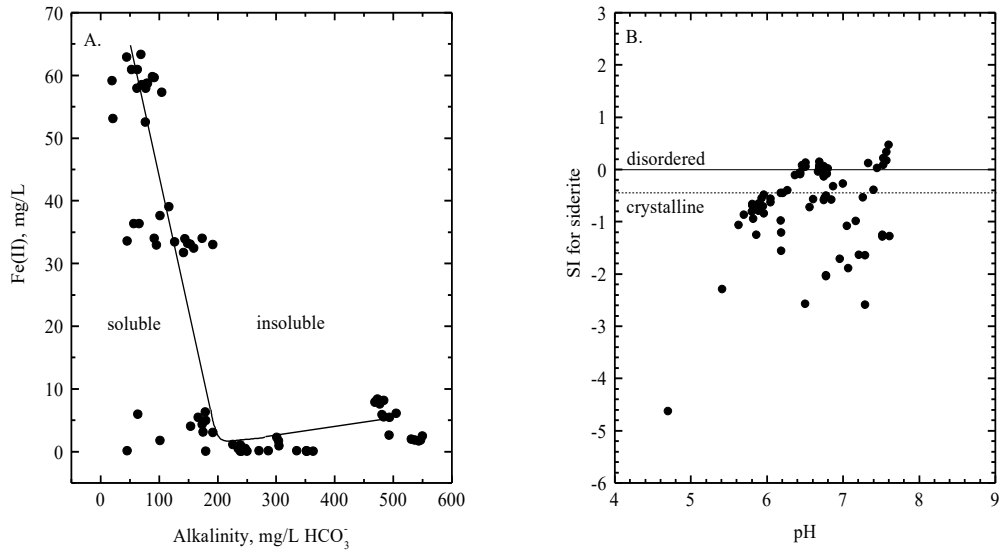

Figure 8. A. Ferrous iron concentration plotted relative to alkalinity (as HCO_3). The line is drawn through data points representing samples that are known to be saturated with respect to siderite. B. SI values for siderite plotted relative to pH. The horizontal lines indicate the range of equilibrium solubility from disordered to crystalline siderite.

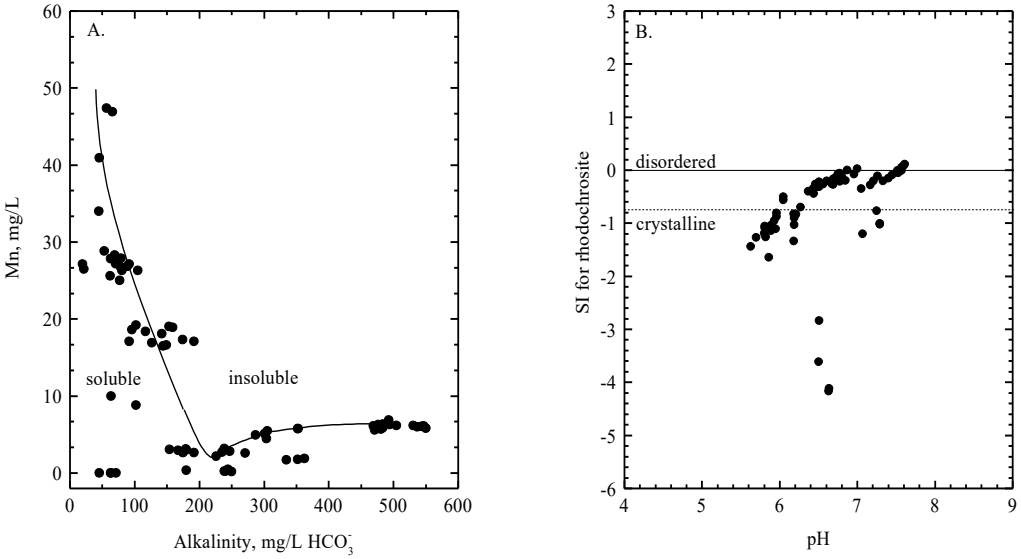

Figure 9.A. Manganese concentrations plotted relative to alkalinity (as HCO_3) with a line drawn through data points representing samples for which rhodochrosite saturation was reached. B. SI values for rhodochrosite plotted relative to pH. The horizontal lines indicate the range of equilibrium solubility from disordered to crystalline rhodochrosite.

Aluminum portrays both conservative and non-conservative behavior depending on pH. Nordstrom and Ball (1986) demonstrated that Al concentrations in many natural systems behaves conservatively at pH values less than about 5, the pK value for the first hydrolysis constant. At or above a pH of 5, hydrolysis causes Al to precipitate as hydroxides and hydroxysulfates. The same behavior appears in the Al data from this project. Figure 10A shows the concentration of Al decreasing with increasing pH, similar to the trend for Fe^{+3} iron, but the concentrations for pH values less than 5 are under-saturated with respect to amorphous $Al(OH)_3$ (left of the solid line). Aluminum concentrations under acidic conditions are shown in Fig. 10B in which a strong correlation with SO_4^{-2} is obtained ($r^2 = 0.93$). The logarithm of the free Al^{+3} ion activity is plotted relative to pH in Fig. 11A and shows that the strongly decreasing activities at pH values greater than 5 correspond to the range for crystalline to amorphous $Al(OH)_3$ solubility. Figure 11B shows the saturation indices for amorphous $Al(OH)_3$ and the tendency for the SI values to be constrained to the range of crystalline gibbsite to amorphous $Al(OH)_3$ saturation for pH values greater than 5.

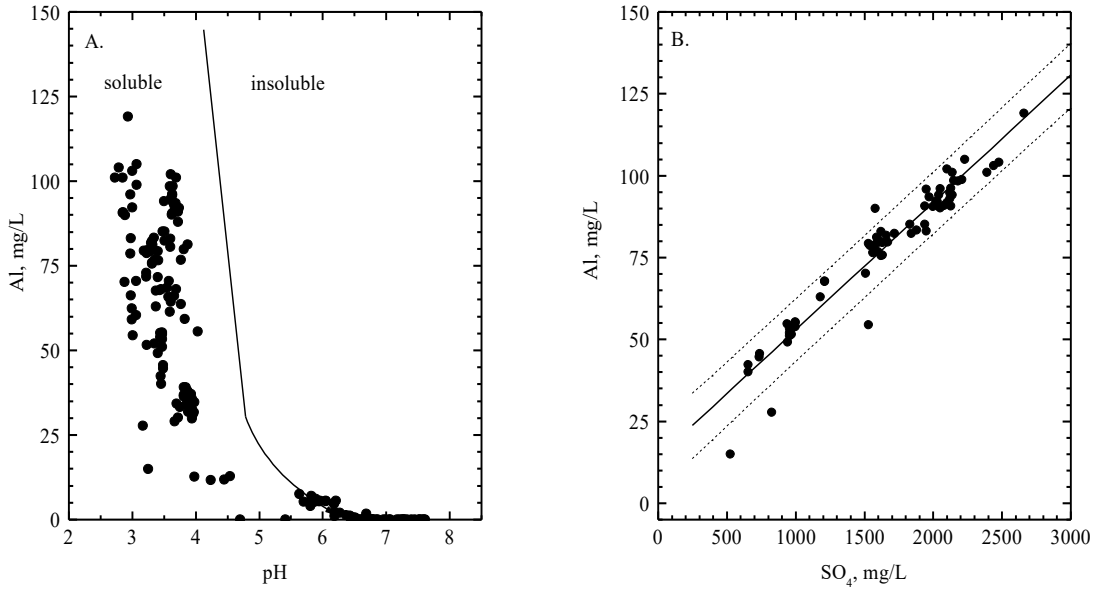

Figure 10.A. Aluminum concentrations plotted relative to pH with a line drawn for amorphous $Al(OH)_3$ solubility. B. Aluminum concentrations plotted relative to SO_4^{-2} concentrations for the acidic waters (pH < 4) of Straight Creek surface drainage and alluvial aquifer.

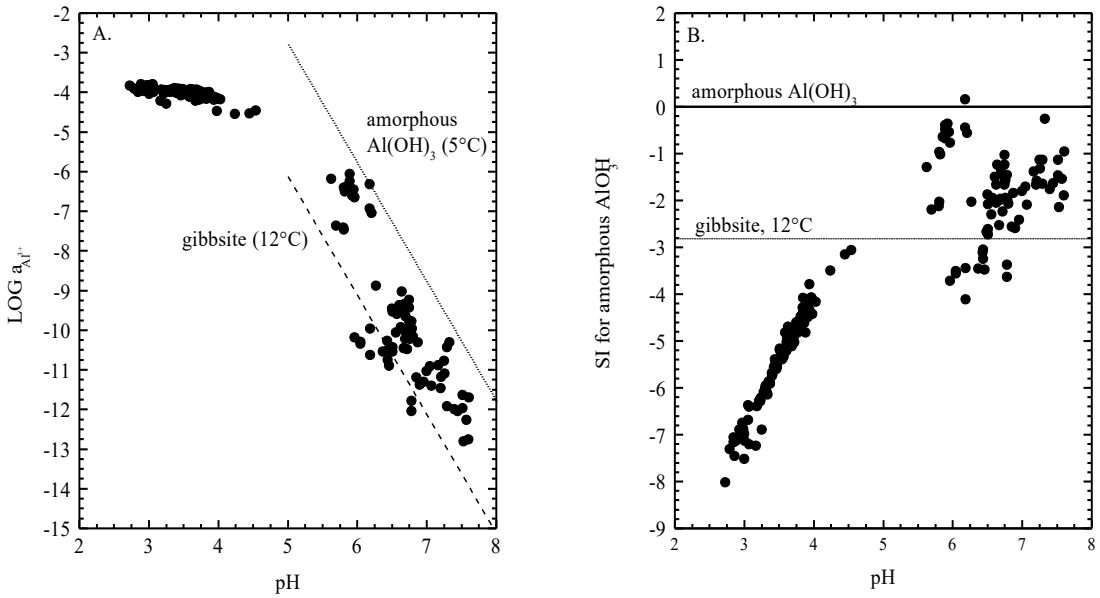

Figure 11. A. Logarithm of the free Al^{+3} ion activity plotted relative to pH with lines drawn for solubility limits of amorphous $Al(OH)_3$ at 5ºC for the maximum and crystalline gibbsite at 12ºC for the minimum. B. SI values for amorphous $Al(OH)_3$ and crystalline gibbsite

Concentrations of calcium are limited by gypsum and calcite mineral saturation. A plot of calcium relative to sulfate concentrations in Fig. 12A indicates an upper limit to Ca concentrations from having reached gypsum saturation. The plot of $Ca:SO_4$ molar ratios relative to pH in Fig. 12B indicates that the water compositions range from those predominantly affected by pyrite oxidation (pH values 2 to 5) to those predominantly affected by calcite and gypsum dissolution (pH values > 5). In Fig. 13A, the saturation indices for gypsum are plotted relative to Ca concentrations and in Fig. 13B the saturation indices for calcite are plotted relative to pH. Gypsum SI values reach saturation and are maintained at equilibrium, whereas calcite SI values go to supersaturation for two possible reasons. One reason is that at the high SO_4^{-2} concentrations found in most of these ground waters, calcite precipitation is inhibited. The other is that gypsum, being a more soluble salt, can likely dissolve more rapidly than calcite can precipitate.

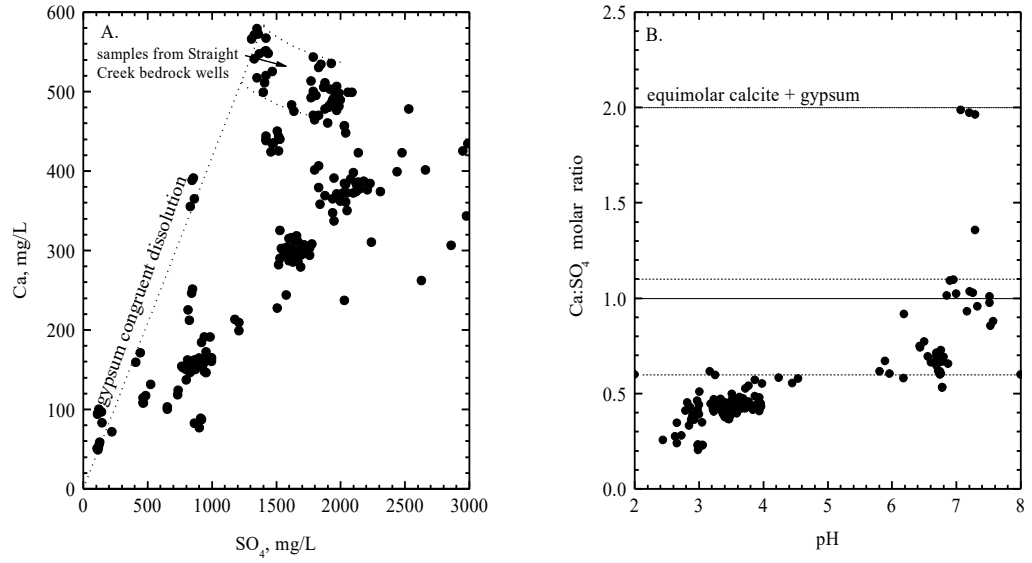

Figure 12. A. Calcium concentrations plotted relative to SO_4^{-2} concentrations showing the gypsum congruent dissolution line (diagonal dashed line) and the range for gypsum solubility. B. Ca:SO_4 molar ratio plotted relative to pH with the solid line for gypsum stoichiometry enveloped by two dashed lines showing the range of gypsum dissolution predominance.

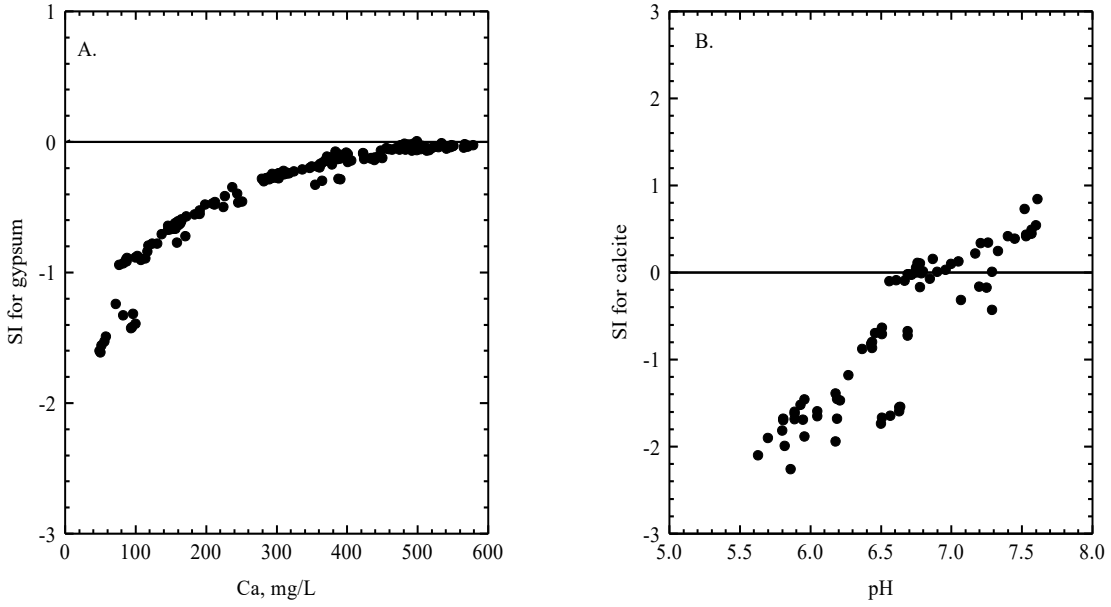

Figure 13. A. SI values for gypsum plotted relative to calcium concentrations. B. SI values for calcite plotted relative to pH.

Barium concentrations are limited by the solubility of the mineral barite, $BaSO_4$, independently of pH. Barium concentrations are plotted relative to SO_4^{-2} concentrations in Fig. 14A. Many samples appear to be supersaturated. The plot of barite SI values plotted in Fig. 14B also shows many data points in the region of supersaturation. One possible reason for supersaturation may be barite colloids were not always filtered out.

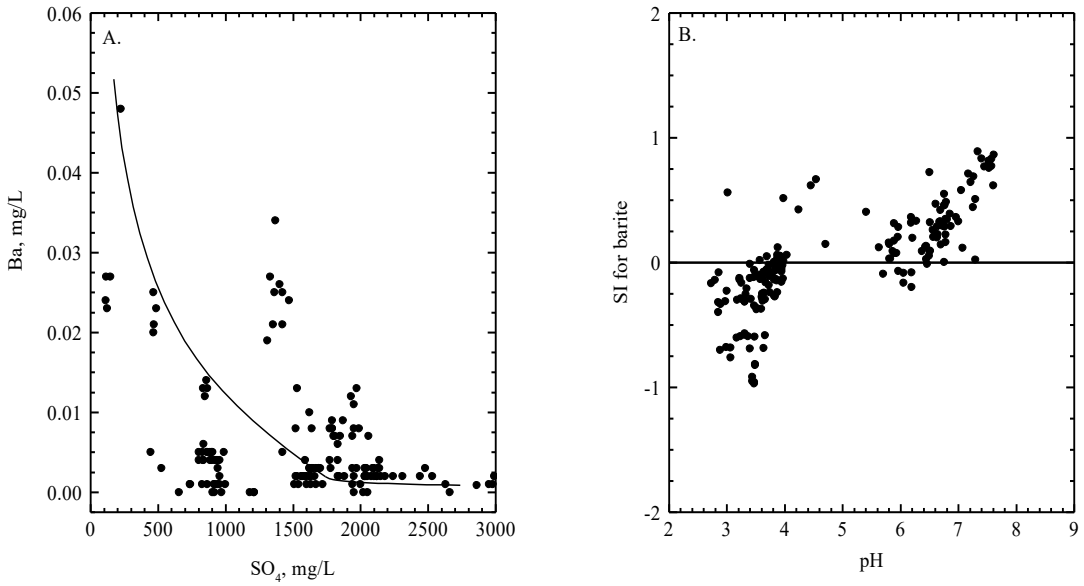

Figure 14. A. Barium concentrations plotted relative to SO_4^{-2} concentrations with a line showing the equilibrium solubility for barite. B. SI values for barite plotted relative to pH.

Acidic waters typically have higher silica concentrations than circumneutral-pH ground waters, although this is not a widely recognized fact. These higher concentrations occur because at low pH aluminosilicate minerals dissolve rapidly whereas silica polymerization and precipitation are slow processes (Dietzel, 2000; Icopini et al., 2005). Consequently, silica concentrations increase with decreasing pH (Fig. 15A). A limit appears to be reached where saturation with respect to amorphous silica is approached at very low pH values (Fig. 15B).

Conclusions

A detailed hydrogeochemical investigation of ground waters in the mineralized region of the Red River Valley of the Sangre de Cristo Mountains in northern New Mexico has resulted in identification of two main types of ground-water chemistry unaffected by mining or other anthropogenic activities. One type is acidic (pH 3 to 4), which contains elevated concentrations of SO_4^{-2}, Fe, Al, Mn, Zn, Cd, Ni, Co, Cr, Cu, Ca, Mg, Be, and F^-, and occurs primarily in debris fans formed from rapidly eroding scar areas containing high concentrations of pyrite in QSP-altered andesite. The other type is circumneutral in pH with elevated concentrations of SO_4^{-2}, Fe,

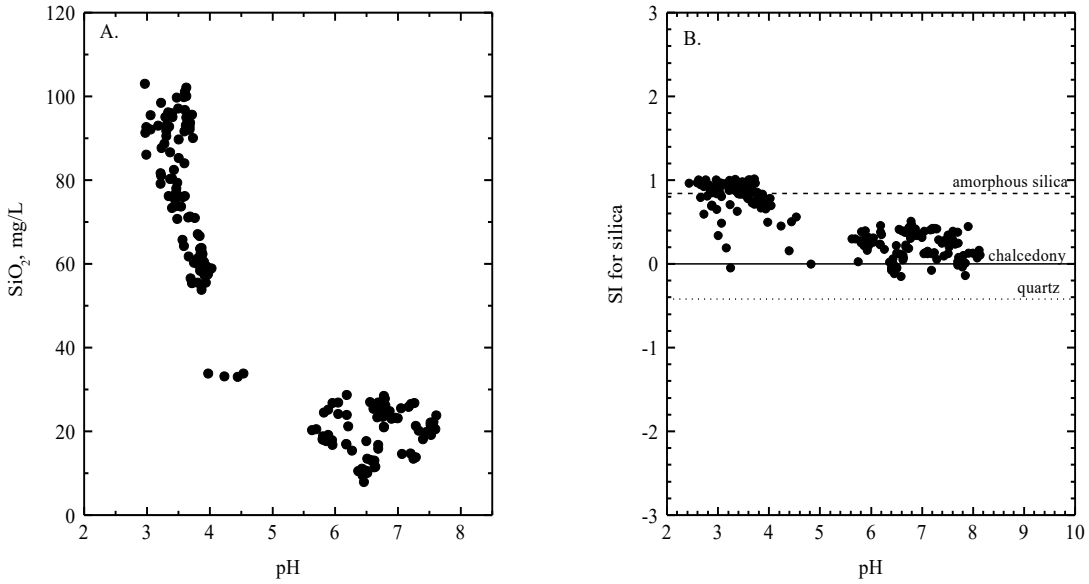

Figure 15.A. Silica concentrations plotted relative to pH. B. SI values for three varieties of silica, amorphous, chalcedony (microcrystalline quartz), and quartz, plotted relative to pH.

Mn, Ca, and Mg and occurs in bedrock. At low pH, most constituent concentrations correlate linearly with SO_4^{-2} concentrations, indicating consistent weathering stoichiometries and conservative behavior during dilution with downgradient transport. The main exception is Fe which, when oxidized, hydrolyzes and precipitates hydrous ferric oxides (or hydroxysulfates) at pH values greater than 2.5. Aluminum behaves conservatively at pH values less than 4 and non-conservatively at pH values greater than 5, with concentrations limited by the solubility of crystalline gibbsite or amorphous $Al(OH)_3$. Both Fe^{+3} iron and Al^{+3} concentrations are controlled by pH because of their tendency to hydrolyze and precipitate.

At higher pH values, Mn and Fe^{+2} iron concentrations are limited by saturation with respect to rhodochrosite and siderite, respectively. Carbonate buffering is available in the bedrock aquifer from carbonate mineralization (calcite, rhodochrosite, and dolomite) and anoxic conditions prevent pyrite oxidation. Calcite and gypsum saturations also are reached in the more mineralized ground waters, placing a limit on Ca, but not Mg, concentrations. Barium concentrations are limited by barite saturation. Silica concentrations increase at low pH but seem to be limited by an amorphous silica phase.

These geochemical trends and mineral solubility controls provide ranges of concentrations that can be expected for natural mineralized conditions, including estimates for pre-mining ground-water quality, in the Red River Valley and could provide a basis for establishing water-quality standards.

References

Alpers, C.N. and Nordstrom, D.K., 2000, Estimation of pre-mining conditions for trace metal mobility in mineralized areas: in Proceedings Fifth International Conference on Acid Rock Drainage, ICARD 2000, v. 1, Society for Mining, Metallurgy, and Exploration, Littleton, Colo., 463-472.

Ball, J.W., Runkel, R.L., and Nordstrom, D.K., 2005, Questa baseline and pre-mining ground-water quality investigation. 12. Geochemical and reactive-transport modeling based on low-flow and snowmelt tracer studies for the Red River, New Mexico: U.S. Geological Survey Scientific Investigations Report 2005-5149.

Caine, J.S., 2003, Questa baseline and pre-mining ground-water quality investigation. 6. Preliminary brittle structural geologic data, Questa Mining District, southern Sangre de Cristo Mountains, New Mexico: U.S. Geological Survey Open-File Report 03-280.

Church, S.E., Fey, D.L., and Marot, M.E., 2005, Questa baseline and pre-mining ground-water quality investigation. 8. Lake-sediment geochemical record from 1960 to 2002, Eagle Rock and Fawn Lakes, Taos County, New Mexico: U.S. Geological Survey Open-File Report 2005-5006.

Dietzel, M., 2000, Dissolution of silicates and the stability of polysilicic acid: Geochimica et Cosmochimica Acta 64, 3275-3281. http://dx.doi.org/10.1016/S0016-7037(00)00426-9.

Fleischer, M., 1955, Minor elements in some sulfide minerals: in Bateman, A.M., ed., Economic Geology, Fiftieth Anniversary Volume, 1905-1955, Part II, Lancaster Press, Lancaster, Penn., 970-1024.

Icopini, G.A., Brantley, S.L., and Heaney, P.J., 2005, Kinetics of silica oligomerization and noncolloid formation as function of pH and ionic strength at 25ºC: Geochimica et Cosmochimica Acta 69, 293-303. http://dx.doi.org/10.1016/j.gca.2004.06.038.

Livo, K.E. and Clark, R. N., 2002, Mapped Minerals at Questa, New Mexico, Using Airbourne Visible-Infrared Imaging Spectrometer (AVIRIS) Data--preliminary report: U.S. Geological Survey Open-File Report 02-0026.

Lovetere, S.H., Nordstrom, D.K., Maest, A.S., and Naus, C.A., 2004, Questa baseline and pre-mining ground-water quality investigation. 3. Historical ground-water quality for the Red River Valley, New Mexico: U.S. Geological Survey Water-Resources Investigations Report 03-4186.

Ludington, S., Plumlee, G.S., Caine, J.S., Bove, D., Holloway, J.M., and Livo, K.E., 2004, Questa baseline and pre-mining ground-water quality investigation. 10. Geologic influences on ground and surface waters in the lower Red River watershed, New Mexico: U.S. Geological Survey Scientific Investigations Report 2004-5245.

Maest, A.S., Nordstrom, D.K., and Lovetere, S.H., 2004, Questa baseline and pre-mining ground-water quality investigation. 4. Historical surface-water quality for the Red River Valley, New Mexico: U.S. Geological Survey Scientific Investigations Report 2004-5063.

McCleskey, R.B., Nordstrom, D.K., Steiger, J.I., Kimball, B.A.,and Verplanck, P.L., 2003, Questa baseline and pre-mining ground-water quality investigation. 2. Low-flow (2001) and

snowmelt (2002) synoptic/tracer water chemistry for the Red River, New Mexico: U.S. Geological Survey Open-File Report 03-148.

McCleskey, R.B. Nordstrom, D.K., and Naus, C.A., 2004, Questa baseline and pre-mining ground-water quality investigation. 16. Quality assurance and quality control of water analyses: U.S. Geological Survey Open-File Report 2004-1341.

Meyer, J. and Leonardson, R., 1990, Tectonic, hydrothermal and geomorphic controls on alteration scar formation near Questa, New Mexico: New Mexico Geological Society Guidebook, 41st Field Conference, Southern Sangre de Cristo Mountains, p. 417-422.

Naus, C.A., McCleskey, R.B., Nordstrom, D.K., Donohoe, L.C., Hunt. A.G., Paillet, F., Morin, R.H., and Verplanck, P.L., 2005, Questa baseline and pre-mining ground-water quality investigation. 5. Well installation, water-level Data, and surface- and ground-water geochemistry in the Straight Creek Drainage Basin, Red River Valley, New Mexico, 2001-03: U.S. Geological Survey Scientific Investigations Report 2005-5088.

Nordstrom, D.K., and Ball, J.W., 1986, The geochemical behavior of aluminum in acidified surface waters: Science 232, 54-56. http://dx.doi.org/10.1126/science.232.4746.54.

Nordstrom, D.K., McCleskey, R.B., Hunt, A.G., and Naus, C.A., 2005, Questa baseline and pre-mining ground-water quality investigation. 14. Interpretation of ground-water geochemistry in catchments other than the Straight Creek catchment, Red River Valley, Taos County, New Mexico, 2002-2003: U.S. Geological Survey Scientific Investigations Report 2005-5050.

Plumlee, G.S., Lowers, H.A., Ludington, S.D., Koening, A.E., and Briggs, P.H., 2005, Questa baseline and pre-mining ground-water quality investigation. 13. Mineral microscopy and chemistry of mined and unmined porphyry molybdenum mineralization along the Red River, New Mexico – Implications for ground- and surface-water quality: U.S. Geological Survey Scientific Investigations Report 2005-1442.

Powers, M.H. and Burton, B.L., 2004, Questa baseline and pre-mining ground-water quality investigation. 1. Depth to bedrock determinations using shallow seismic data acquired in the Straight Creek Drainage near Red River, New Mexico: U.S. Geological Survey Open-File Report 2004-1236.

Questa, 2005, Questa baseline and pre-mining ground-water quality investigation, Red River Valley Basin, New Mexico, available on the World Wide Web, accessed December 19, 2005, at URL

http://wwwbrr.cr.usgs.gov/projects/GWC_chemtherm/questa.htm

Runnells, D.D., Shepard, T.A., and Angino, E.E., 1992, Metals in water–Determining natural background concentrations in mineralized areas: Environmental Science and Technology 26, 2316-2322. http://dx.doi.org/10.1021/es00036a001

To, T.B., Nordstrom, D.K., Cunningham, K.M., Ball, J.W., and McCleskey, R.B., 1999, New method for the direct determination of dissolved Fe(III) concentration in acid mine waters: Environmental Science and Technology 33, 807-813. http://dx.doi.org/10.1021/es980684z.